

Correlations in laser-induced electron-positron pair creation

K. Krajewska* and J. Z. Kamiński

Institute of Theoretical Physics, Faculty of Physics, University of Warsaw, Hoża 69, 00-681 Warszawa, Poland

(Received 19 May 2011; published 26 September 2011)

Probability rates of electron-positron pair creation in head-on laser-beam-proton collisions are investigated, using an exact treatment of the colliding proton as a finite-mass particle. We observe that the recoil effects become more important when passing from the perturbative multiphoton regime to the nonperturbative above-threshold regime of laser-matter coupling. Thus we concentrate on the latter case. In this regime, our detailed analysis shows that energy supplied by the colliding proton makes the process more effective, and that the electrons and positrons that are created during the collision are more energetic than in the case when the momentum transfer from the proton is neglected. A number of similarities to above-threshold atomic ionization are also illustrated.

DOI: [10.1103/PhysRevA.84.033416](https://doi.org/10.1103/PhysRevA.84.033416)

PACS number(s): 34.50.Rk, 32.80.Wr, 12.20.Ds

I. INTRODUCTION

The possibility of converting energy into mass, as being fundamental in relativistic quantum theory [1–3], led Sauter [4], and later also Schwinger [5], to their prediction of electron-positron pair production from a vacuum in the presence of a static electric field. In this case, the electric field necessary to observe the e^-e^+ pairs turned out to be $E_{\text{cr}} = 1.3 \times 10^{16}$ V/cm, which was far too high to perform the respective experiment in a laboratory. A similar conclusion was reached when the electron-positron pair creation from a vacuum in an alternating electric field was studied [6,7]. Importantly, with the presently available very powerful laser sources such as near-visible lasers working at intensities 10^{22} W/cm² [8,9], and yet more powerful optical lasers built within the European Light Infrastructure project [10], pair creation from a vacuum is becoming feasible in the laboratory. Let us note that for contemporary femtosecond laser pulses, it is justified to describe them theoretically by electromagnetic plane waves, though there have been very recent attempts to go beyond this approximation, particularly when describing Compton and Thomson scattering [11–16]. At this point, one has to realize that a single plane-wave laser field cannot extract any e^-e^+ pairs from the vacuum, no matter how strong the laser field is [5]. For this reason the assistance of a Coulomb field [17–38], a nonlaser photon [39–43], or multiple laser beams [44–51], is necessary.

Despite all of the above-mentioned theoretical works, there has been only one experiment performed so far, in which the laser-induced electron-positron pair creation was observed [52,53]. In this experiment, a highly relativistic electron beam was rescattered by an intense optical laser producing a very energetic photon, which then recollided with the laser beam to produce pairs. Since the production of a real photon was highly reduced in this process, one may expect that a direct process would be far more efficient.

The direct process that we have in mind was considered for the first time by Yakovlev in Ref. [17]. In this paper, Yakovlev analyzed the electron-positron pair creation by the impact of a circularly polarized laser wave on a nucleus at rest. The same process for a linearly polarized light was later considered by

Mittleman [18]. It follows from both of these investigations that the rates of pair creation in such a configuration are indeed very small. To make them significantly higher, the motion of a target particle must be accounted for [20–25,28–38]. It was noted by Müller and co-authors [20–22] that if the target particle is counterpropagating toward the laser beam at a large Lorentz factor γ , then in its rest frame both the laser frequency and the laser-field strength are enhanced by roughly 2γ . In other words, for presently available superintense laser pulses, the electric field experienced by the target particle during its collision with the laser beam approaches the critical Schwinger value E_{cr} . This makes it possible to observe the electron-positron pairs.

It is frequently emphasized that pair creation in ultrastrong laser fields shows similarities to strong-field ionization of atoms [54–56]. There is a threshold energy that must be overcome in order for both of these processes to be observed; while in the case of ionization the electron has to overcome the ionization potential, thus for the e^-e^+ pair creation the respective threshold is twice the rest energy of the electron, $2m_e c^2$ (here m_e is the electron mass). This, however, applies only for weak fields, while for stronger laser fields these thresholds are substantially modified. In both cases, if the threshold energy is greater than a laser frequency, we can talk about different-order-photon processes leading to ionization or pair creation. It is well known that there are different regimes of laser-matter interaction leading to ionization, and that these regimes can be distinguished with the help of the Keldysh adiabaticity parameter, ξ [57]. Similarly, in a relativistic domain one can introduce a parameter,

$$\mu = \frac{|eA_0|}{m_e c}, \quad (1)$$

where A_0 is the amplitude of a laser field and e is the electron charge ($e < 0$). In fact, it was shown in Ref. [56] that $\mu = 1/\xi$. The parameter μ , which is relativistically invariant, allows one to distinguish different regimes of laser-matter interaction leading to pair creation [54–56]. In the multiphoton regime of pair creation, for which $\mu \ll 1$, the lowest-order-photon process of pair creation is dominant. When $\mu \sim 1$ we deal with the so-called above-threshold regime, whereas for $\mu \gg 1$ we are in the tunneling regime of laser-matter coupling. In general, for $\mu \gtrsim 1$ the higher-order-photon processes resulting

*katarzyna.krajewska@fuw.edu.pl

in pair creation become important, and thus the probability rates cannot be treated perturbatively in terms of μ .

In this paper, we consider the electron-positron pair creation in laser-beam-proton collisions in the above-threshold interaction regime (for $\mu \sim 1$), which is complementary to previous theoretical investigations [20–25,28–38]. Additionally, in most theoretical works mentioned here, the colliding particles were assumed to be infinitely heavy, and thus the recoil effects imparted on them were neglected. Here we shall go beyond this approximation.

In light of the present paper, it is important to mention papers by Müller and Müller [32], and by ourselves [34,38], where a complete description of laser-induced pair creation with an exact account for the recoil of target particles was presented. While in Ref. [32] the authors considered the perturbative multiphoton regime of pair creation, we analyzed the process in the fully unperturbative tunneling regime [34,38]. It follows from Ref. [32] that the recoil effects are negligibly small for such laser-field parameters so that one deals with the multiphoton pair creation in a deeply perturbative domain ($\mu = 7.5 \times 10^{-4}$). On the other hand, we demonstrated that in the tunneling domain (for $\mu = 10^2$) the probability rates of e^-e^+ pair production increase tremendously owing to the nuclear recoil [34,38]. In addition, we showed a dramatic dependence of the corresponding probability rates on the polarization of the laser wave impinging on the target [34], which is in contrast to what is observed in the multiphoton regime. Because multiphoton and tunneling pair creation are very distinct, even though they are two limiting cases of the same process, we find interesting to consider the intermediate regime of above-threshold pair creation. The purpose here is to investigate the role of recoil effects on efficiency and qualitative features of the process. In particular, we are interested in the following: (a) How do the recoil effects influence the probability rates of pair production? (b) What are typical above-threshold pair creation spectra in this regime; can one observe clear similarities with the above-threshold atomic ionization? (c) What are the correlations between the target and the product particles, or the product particles themselves? In the present paper, we provide answers to these questions by analyzing process of e^-e^+ pair creation in laser-beam-proton collisions, which is along the lines presented in Refs. [23–25,28,34,38].

This article will be organized as follows. In Sec. II, we shall briefly summarize the main results regarding the theory of electron-positron pair creation in laser-beam-proton collisions that we have derived in our previous works for an arbitrary target particle [23–25,28,34,38], and that we will use in the current paper as well. Also in Sec. II we shall formulate the scheme of calculating coarse-grained probability rates of e^-e^+ pair creation. In the following sections (Secs. III–VI), we shall present numerical examples for the corresponding probability rates. Section VII will be devoted to a summary of our results and to some final remarks.

II. THEORY

The process of electron-positron pair creation in head-on laser-beam-proton collisions is investigated in this paper in the first-order Born approximation (without the radiative

corrections). We describe the laser field by a monochromatic, linearly polarized plane wave of polarization four-vector $\varepsilon = (0, \mathbf{e})$, such that $\varepsilon^2 = -1$ and $\mathbf{e}^2 = 1$, and its strength described by A_0 . More precisely, we represent the laser field by the four-vector potential,

$$A^\mu(k \cdot x) = A_0 \varepsilon^\mu \cos(k \cdot x), \quad (2)$$

with the wave four-vector $k = (\omega/c)(1, \mathbf{n})$; here, ω is the frequency of field oscillations while $\mathbf{n} = -\mathbf{e}_z$ is the direction of propagation of the plane wave. In the following, we compare the results for both situations when the colliding proton is treated as an infinitely heavy particle, and so the recoil imparted on it is neglected (the so-called potential approximation) with the situation when the finite mass of the proton is accounted for. To make such a comparison meaningful, we give all the quantities and the results presented for the latter case in the reference frame where the proton is at rest outside of the laser focus, long before the collision takes place. Unless otherwise stated, we keep in the following $\omega = m_e c^2$ and $\mu = 1$.

We use the notation and mathematical convention introduced in our recent papers on the electron-positron pair creation [34,38]. In particular, in all formulas below we keep $\hbar = 1$; however, our numerical results are presented either in arbitrary units, or in relativistic units such that $c = m_e = 1$.

A. Probability rates of pair creation

We take over from our earlier works [34,38] the derivation of probability rates of electron-positron pair creation in laser-beam-proton collisions, with an exact account for a proton recoil. However, for the convenience of the reader, we reproduce the main result here. The total probability rate of e^-e^+ pair creation W has been defined as a sum over all N -photon partial rates W_N , which are defined by

$$W \equiv \sum_N W_N = \sum_N \int d^3 q_f d^3 p_{e^-} d^3 p_{e^+} \sum_{\{\lambda\}} \frac{Z^2 \alpha^2 m_e^2 m_p^2 c^9}{2\pi^3} \times \frac{|t_N|^2}{E_{q_i} E_{q_f} E_{p_{e^-}} E_{p_{e^+}}} \delta(\bar{q}_i - \bar{q}_f - \bar{p}_{e^-} - \bar{p}_{e^+} + Nk). \quad (3)$$

Here the integration is over the final proton momentum, \mathbf{q}_f , and also over the electron and the positron momenta, \mathbf{p}_{e^-} and \mathbf{p}_{e^+} , respectively. $\sum_{\{\lambda\}}$ in Eq. (3) denotes averaging with respect to the initial spin degrees of freedom and summation over the final spin degrees of freedom of all particles. Here m_p is the proton mass, and the δ function defines the dressed four-momentum conservation condition, whereas t_N is the N th order matrix element,

$$t_N = \sum_L C_{N-L}^\mu \tilde{D}_{\mu\nu}(\bar{q}_i - \bar{q}_f + Lk) \mathcal{F}_L^\nu. \quad (4)$$

The summation in Eq. (4) is with respect to the number of laser photons L , which are exchanged between the proton and the field. The coefficients C_{N-L}^μ and \mathcal{F}_L^ν can be derived from the Fourier expansion of the proton and the pair four-currents, but we do not present their explicit form here (see Ref. [34] for the formulas and the details of derivations). From the point of view of this paper, it is more important to realize that the Fourier transform of the photon propagator, which is present

in Eq. (4),

$$\tilde{\mathcal{D}}_{\mu\nu}(\bar{q}_i - \bar{q}_f + Lk) = -\frac{g_{\mu\nu}}{(\bar{q}_i - \bar{q}_f + Lk)^2}, \quad (5)$$

has poles when $(\bar{q}_i - \bar{q}_f + Lk)^2 = 0$. These divergences are the source of the so-called Oleinik resonances [38,58–60], but they can be turned into finite resonances when a finite pulse, instead of a plane wave, is considered. In doing so, we apply a similar regularization procedure as used in Ref. [35]; in Eq. (5), we replace $1/Q^2$ by $1/(Q^2 + i\epsilon)$, where in our case the regularization parameter ϵ is related to the length of the laser pulse. More precisely, we take $\epsilon = 2k^0/c\tau$, where the pulse length is $\tau = 2\pi n_{\text{osc}}/\omega$, whereas n_{osc} is the number of laser pulse oscillations. At this point, let us note that all the results that are presented in this paper have been obtained for $n_{\text{osc}} = 5$; however, we have also checked that for $n_{\text{osc}} = 15$ the results do not change significantly. At this point, let us also mention that using our exact treatment of the colliding target particle, we have analyzed recently the effect of dressing it by the laser field on the probability rates of pair production [34,38]. We have found that for the very many photon processes, the photon exchange between the laser field and the target particle is not that essential. The same stays true for few photon processes and for the parameters considered in this paper. Thus we shall present the results for $L = 0$.

Even though the above formulas have been obtained using a more accurate approach of treating the colliding proton as a finite-mass particle [34,38], for completeness, we present now the respective expression for the case when the proton is treated as an infinitely heavy particle, in which case one can disregard its recoil by the laser beam [23–25,28].

B. Probability rates of pair creation in an infinitely heavy proton approximation

It follows from our previous works [23–25,28] that the total probability rate of e^-e^+ pair creation in laser-beam-proton collisions W in the potential approximation is given as

$$W \equiv \sum_N W_N = \sum_N \int d^3 p_{e^-} d^3 p_{e^+} \sum_{\{\lambda\}} \frac{Z^2 \alpha^2 m_e^2 c^5}{2\pi^3} \frac{1}{E_{p_{e^-}} E_{p_{e^+}}} \times \frac{|M_N|^2}{(\bar{\mathbf{p}}_{e^-} + \bar{\mathbf{p}}_{e^+} - N \frac{\omega}{c} \mathbf{n})^4} \delta\left(\bar{p}_{e^-}^0 + \bar{p}_{e^+}^0 - N \frac{\omega}{c}\right). \quad (6)$$

This equation also defines the partial probability rates of pair creation W_N . In Eq. (6), $\sum_{\{\lambda\}}$ stands for the summation over the final spin degrees of freedom, whereas the δ function expresses the energy conservation law. M_N is the matrix element that follows from the Fourier decomposition of the pair four-current (see, for instance, Ref. [23] for its exact form). Let us note that this time the probability rates introduced in Eq. (6) do not diverge, as the equation $\bar{\mathbf{p}}_{e^-} + \bar{\mathbf{p}}_{e^+} = N \frac{\omega}{c} \mathbf{n}$ has no solutions that satisfy the corresponding energy conservation law.

C. Coarse-grained probability rates of pair creation

In the subsequent sections, we shall investigate correlations in probability rates of above-threshold e^-e^+ pair production. Based on Eq. (3) in the case when the proton recoil is taken into account, or on Eq. (6) if it is not, we shall calculate the

coarse-grained differential rates of pair creation and we will analyze their dependence on two correlated quantities. For now, let us call these quantities x and y .

A general procedure of calculating the coarse-grained differential rates of pair creation starts with computing the sextuple-differential partial rates, which follows from Eqs. (3) and (6). In both formulas, because of the presence of the δ functions, we are left with only six independent variables, one of them being discrete and the rest continuous. This schematically can be written as

$$W = \sum_N \int d^5 z \frac{d^5 W_N}{dz_1 dz_2 dz_3 dz_4 dz_5}, \quad (7)$$

where z_i ($i = 1, \dots, 5$) are the respective independent variables chosen among spherical coordinates of the momenta \mathbf{p}_{e^-} , \mathbf{p}_{e^+} , and \mathbf{q}_f . To make the notation more compact, we rewrite Eq. (7) as

$$W = \int d^6 z \frac{d^6 W}{dz_1 dz_2 dz_3 dz_4 dz_5 dz_6}, \quad (8)$$

where the sextuple-differential probability rate has been defined,

$$\frac{d^6 W}{dz_1 dz_2 dz_3 dz_4 dz_5 dz_6} = \sum_N \delta(z_6 - N) \frac{d^5 W_N}{dz_1 dz_2 dz_3 dz_4 dz_5}. \quad (9)$$

In Eq. (8), let us distinguish between the chosen variables x and y , and the others,

$$W = \int dx dy d^4 z \frac{d^6 W}{dx dy dz^4}. \quad (10)$$

When calculating $\frac{d^6 W}{dx dy dz^4}$ in the above equation, we use 10^8 – 10^9 sample points, similar to the Monte Carlo method developed in Ref. [24]. In the next step, we divide both intervals where the variables x and y change into equal steps; for instance, the i th interval for the variable x would be $[x_i, x_{i+1}]$, where $x_{i+1} - x_i = \Delta x = \text{const}$, and similarly for y . In the case when x or y is discrete, we choose for the corresponding interval $[N_i - 1/2, N_i + 1/2]$, and so $\Delta N = 1$. We take a rectangular P_{ij} such that the variable x lies in the i th interval and y in the j th interval, and we sum all rates corresponding to the points lying within P_{ij} . This way we obtain the coarse-grained differential rate,

$$\left\langle \frac{d^2 W}{dx dy} \right\rangle_{ij} = \mathcal{A} \int_{x_i}^{x_{i+1}} dx \int_{y_j}^{y_{j+1}} dy \int d^4 z \frac{d^6 W}{dx dy dz^4}. \quad (11)$$

Here \mathcal{A} is a normalization constant chosen such that

$$\sum_{i,j} \left\langle \frac{d^2 W}{dx dy} \right\rangle_{ij} = 1, \quad (12)$$

as we are interested in the relative change of the coarse-grained differential probability rates. To obtain absolute values of the corresponding rates, it is enough to multiply the above distributions by the total probability rate of pair creation, calculated by the Monte Carlo method along the lines presented in Ref. [24]. In case one would like to investigate the dependence of the

coarse-grained rates as a function of only one variable, for instance, x , we define,

$$\left\langle \frac{dW}{dx} \right\rangle_i = \sum_j \left\langle \frac{d^2W}{dx dy} \right\rangle_{ij}. \quad (13)$$

At this point let us also note that one can interpret the coarse-grained differential rates introduced above as the average with respect to two or one variable probability rates of e^-e^+ pair creation. This will be illustrated in the subsequent sections.

III. TOTAL RATES OF PAIR CREATION

Before we proceed with analyzing the laser-induced electron-positron pair creation in the exclusively above-threshold regime, we demonstrate first the corresponding results for different values of the parameter μ , going from the multiphoton ($\mu \ll 1$), up to the above-threshold ($\mu \sim 1$) regime. As was mentioned, all the results are presented for a linearly polarized laser field, which is in contrast to Ref. [32] where a circularly polarized laser field was considered. In Fig. 1 we present the total probability rates for the e^-e^+ pair creation in laser-beam-proton collisions, obtained within the

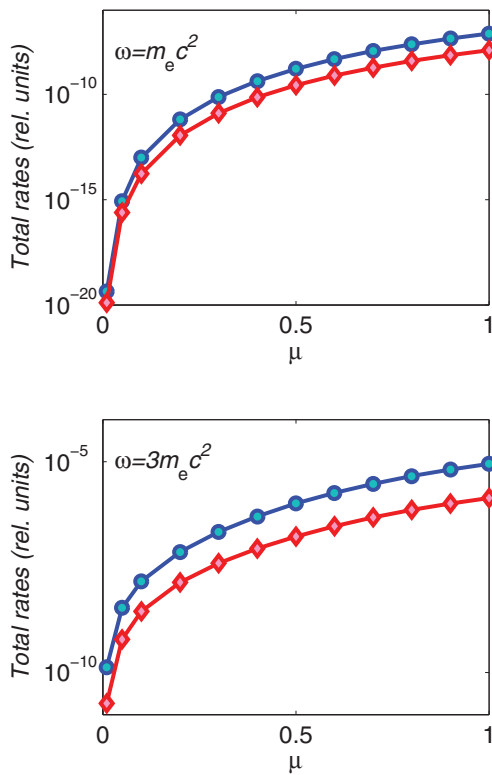


FIG. 1. (Color online) Total probability rates for the e^-e^+ pair production in the course of laser-beam-proton collision as a function of the parameter μ . In both panels we compare the results obtained for the case when the proton recoil is taken into account (blue circles), as was introduced in Refs. [34,38], with the results corresponding to the case when one neglects the proton recoil (red diamonds), as discussed in Refs. [23–25,28]. The results in the upper panel are for $\omega = m_e c^2$, and in the lower panel for $\omega = 3m_e c^2$ (in the reference frame under consideration). The symbols are connected by the lines to guide an eye.

Monte Carlo approach that we have developed in Ref. [24]. Two cases are considered here, namely, when in the chosen reference frame the laser-field frequency is either $\omega = 3m_e c^2$ (lower panel) or $\omega = m_e c^2$ (upper panel). In the first case, one laser photon is enough to create electron-positron pairs, while in the second case at least three photons are necessary in order to do so. In both cases, we compare the results obtained using our exact approach of treating the colliding proton [34,38] (blue circles, upper line) with the results obtained within the infinitely massive proton approximation [23–25,28] (red diamonds, lower line). One can see in both cases the enhancement of the total probability rates of pair creation, if the finite mass of the colliding particle is accounted for. The difference, however, is not that pronounced as in the tunneling regime, which was investigated in Refs. [34,38] for much smaller ω . The point being that, in the case considered in Refs. [34,38], the momentum transfer from the colliding particle made the number of absorbed laser photons significantly smaller, resulting in a tremendous increase of probability rates of e^-e^+ pair production. For a few photon pairs production, which is under investigation now, this is not the case. Let us emphasize that our findings coincide with the results reported in Refs. [32,34,38]. With decreasing the parameter μ , we can see from Fig. 1 that the recoil effects become less important, as was found in a deeply multiphoton regime [32]. On the other hand, for μ having a value around unity, there can be up to one order of magnitude difference between the probability rates for the case when one accounts for, or one disregards, the proton recoil. With still increasing μ (and for smaller ω), the respective difference can even reach a few orders of magnitude, which was shown in Refs. [34,38].

IV. PARTIAL RATES OF PAIR CREATION

When calculating total probability rates of e^-e^+ pair creation in laser-beam-proton collisions (Sec. III), the summation over all N -photon processes, where N is a net number of photons exchanged by the laser field with a pair or with a proton, was carried out (for more details on theoretical methods used in this context, see Refs. [23–25,28,34,38]). In this section, we concentrate on analyzing partial probability rates of electron-positron pair creation W_N , which are due to absorption of different numbers of photons [for the definition of W_N , see Eqs. (3) and (6)].

As was mentioned in the Introduction, the e^-e^+ pair creation shows similarities to strong-field atomic ionization. Because of a nonlinear response to strong laser fields, atomic systems can be ionized with absorption of more photons than a required minimum, a phenomenon known as above-threshold ionization (ATI) [61] (see also Refs. [62–65]). In essence, the ATI spectrum consists of two distinct parts, the origin of which is explained by the three-step model [66,67]. The so-called direct electrons are ionized without further interaction with the parent ion, and they contribute to the low-energy part of the ATI spectrum, which comprises a sequence of peaks decreasing in magnitude with increasing electron energy. The high-energy ATI spectrum consists of peaks of roughly comparable intensities forming the so-called plateau, which originates from the rescattering of ionized electrons by the ionic core under the influence of the laser field. Below we

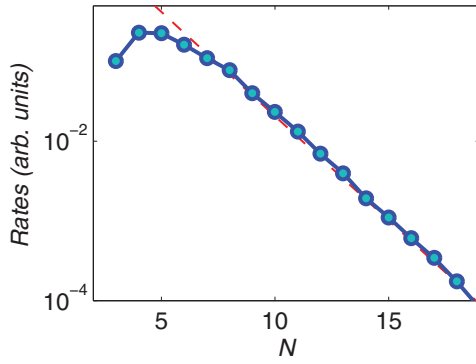


FIG. 2. (Color online) Partial probability rates of electron-positron pair creation in laser-beam-proton collisions for the case when a finite mass of the proton is taken into account (blue circles). The red dashed line marks the fit of these results to the perturbation theory prediction. The laser-field parameters are such that $\omega = m_e c^2$ (in the chosen reference frame) and $\mu = 1$.

present our numerical results for above-threshold pair creation, with an emphasis on analogies with the ATI process described here.

In Figs. 2 and 3, we present the N -photon probability rates of above-threshold electron-positron pair creation (blue circles) for different N [$3 \leq N \leq 18$ (Fig. 2) and $3 \leq N \leq 17$ (Fig. 3)], and for laser-field parameters considered in this paper. While the results shown in Fig. 2 were obtained using a more accurate approach of treating the colliding proton as a finite mass particle [34,38], the rates presented in Fig. 3 were calculated within the infinitely heavy-proton approximation [23–25,28]. Let us note that the presented data resemble a typical low-energy ATI spectrum discussed above. The reason is that we apply here the Born approximation in which the rescattering effects are neglected, resulting in a steep decrease of partial rates with increasing the photon number N . This monotonic behavior is not obeyed for the lowest photon orders, which is also true for the ATI spectra. One can conclude that this is the signature of the above-threshold regime for both ionization and pair creation processes. For comparison, we calculated similar spectra for the laser-field parameters $\omega = m_e c^2$ and $\mu = 0.01$, which is in the multiphoton regime. In this perturbative case, a dominant rate corresponds to the first above-threshold photon process

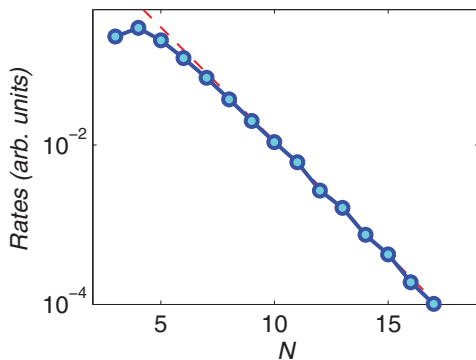


FIG. 3. (Color online) Same as in Fig. 2 but for the case when the colliding proton is assumed to be an infinitely massive particle.

and is followed by a monotonic decrease of subsequent partial rates. It also follows from here, that by increasing the laser field intensity (increasing μ), the largest peak in the spectrum is shifting toward higher photon number N . This resembles, in fact, the so-called peak switching, which has been observed for the ATI electron spectrum [68–71]. We need to mention that in both figures (Figs. 2 and 3) the perturbation theory predictions according to which the partial probability rates of pair production W_N satisfy the power law,

$$W_N \simeq \left(\frac{\mu}{\mu_{\text{th}}} \right)^{2N}, \quad (14)$$

are also marked (dashed red lines). For high enough photon orders N , we observe very good agreement between our results and the theoretical predictions governed by Eq. (14). Our fit shows that $\mu_{\text{th}} = 1/0.74$ and $\mu_{\text{th}} = 1/0.72$ for the data presented in Figs. 2 and 3, respectively. Thus, the difference between both data sets is hardly noticeable for higher N . For lower N , one can see from Figs. 2 and 3 that in the case when the recoil of a colliding proton is taken into account (Fig. 2), the rates are more distinct from the perturbation theory prediction than in the case when the proton recoil is neglected (Fig. 3). One needs to understand that these low partial rates make the biggest contribution to the total probability rate of pair production.

V. DIFFERENTIAL PARTIAL RATES OF PAIR CREATION

In this section, we present the differential partial rates of e^-e^+ pair creation in laser-beam-proton collisions, only for the case that accounts for the proton recoil. The rates are calculated along the lines described in Secs. II A and II C, and for the parameters of the laser field considered in this paper. Let us note that in Fig. 4 and in the subsequent figures, $|\mathbf{q}_f| \equiv |\mathbf{q}_i - \mathbf{q}_f|$ is the momentum transfer from the colliding proton (in the chosen reference frame, where $\mathbf{q}_i = \mathbf{0}$). For the parameters considered in this paper, it happens that the probability rates of pair creation are negligibly small for $N > 20$ and for the momenta $|\mathbf{q}_f|$, $|\mathbf{p}_{e^-}|$, and $|\mathbf{p}_{e^+}|$ bigger than

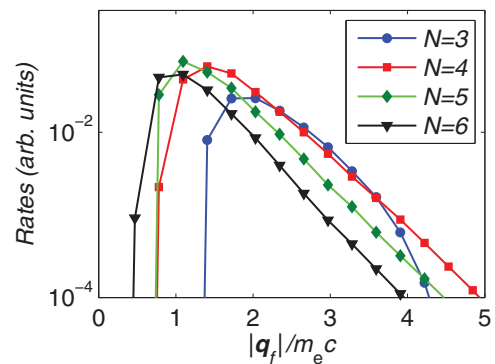


FIG. 4. (Color online) Coarse-grained partial probability rates of electron-positron pair creation as functions of the final proton momentum $|\mathbf{q}_f|$, measured outside of the laser focus. The laser-field parameters are the same as in Fig. 2. The symbols are connected by the lines to guide an eye.

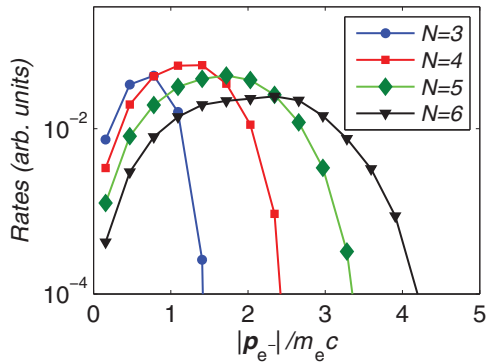


FIG. 5. (Color online) Coarse-grained partial probability rates of electron-positron pair creation as functions of the electron momentum $|\mathbf{p}_{e^-}|$. The laser-field parameters are the same as in Fig. 2. The symbols are connected by the lines to guide an eye.

$20m_e c$. Thus we perform all corresponding integrals defined in Sec. II A using these values as the upper bounds.

In Figs. 4 and 5, one can see the dependence of coarse-grained partial rates of electron-positron pair creation on the target and the product particle momenta, respectively. Each of the rates have been averaged over the momentum interval $20/64 m_e c$. One can observe in Fig. 4 that for a small momentum transfer from the colliding proton, the partial rates grow, but after reaching their maximal values they start to monotonically decrease. For large $|\mathbf{q}_f|$ and $N = 4, 5$, and 6, this dependence is quite well described by the function $\sim \exp(-a_N |\mathbf{q}_f|)$, where $a_N \simeq 2$. A similar behavior of the partial rates as a function of the electron (or positron) momentum is observed in Fig. 5. This time the corresponding dependence on $|\mathbf{p}_{e^-}|$ can be approximated by the function $\sim \exp(-b_N (|\mathbf{p}_{e^-}| - p_N)^{c_N})$, where p_N corresponds to the maximum of the curves shown in Fig. 5, whereas $c_N \simeq 3$. In both figures, one sees also a kind of “peak switching” of the differential partial rates, depending on the proton (Fig. 4) or the product particle (Fig. 5) momentum. The difference is that, while the highest peak in the spectrum is being gradually switched to higher electron (positron) momentum with increasing number of absorbed laser photons N (Fig. 5), the “peak switching” toward lower momentum transfer from the proton (with increasing N) is observed in Fig. 4. This can be explained if one notes that in order to produce the electron-positron pairs, there must be energy supplied either by the laser field, or by the proton. Therefore absorption of more above-threshold photons from the laser field makes it possible to produce more energetic electrons and positrons. At the same time, the higher-order processes become more efficient when the energy supplied by the proton during its collision with the laser field decreases.

In closing this section, let us mention that for the case considered in this paper we have also analyzed angular distributions of created pairs. We have noted that, when the finite mass of a proton is accounted for, in the reference frame chosen in this paper the electrons and the positrons are preferably created in the plane spanned by the laser-field polarization and the laser-field propagation directions. In addition, the particles are created in the direction of the laser-beam propagation. These seem to be typical features of the pair

creation process that are observed also in the tunneling regime of the laser-matter interaction when the recoil effects are neglected (see, for instance, Ref. [3] and references therein).

VI. COARSE-GRAINED DIFFERENTIAL RATES OF PAIR CREATION

In Fig. 6 we present coarse-grained differential probability rates of e^-e^+ pair creation, defined by Eq. (11), as functions of either (a) the number of absorbed laser photons and the momentum transfer from the colliding proton (left panel) or (b) the photon number and the momentum picked up by the electron (or positron) (right panel). The momenta shown in both panels change from 0 to $20m_e c$, and these intervals have been divided into 64 pieces each. For visualization, the respective rates are raised to the power $1/10$ so the areas where the rates are small can be better seen. The presented results are for the laser-field parameters considered in this paper, and they have been obtained using the theoretical approach that accounts for a finite mass of a colliding proton. It is clearly seen from the left panel that the maximum rate of pair production lies in the range where the momentum kick from the proton varies roughly from $m_e c$ to $2m_e c$. For a zero momentum transfer, the rates are negligibly small. In addition, we observe that the lowest-order photon process is less effective than the subsequent processes, in particular than the fourth- up to the seventh-photon processes. This is a typical nonperturbative dependence of the probability rates of pair creation on the number of laser photons absorbed from the field N . On the other hand, it follows from the right panel of Fig. 6 that with increasing the number of absorbed photons N more energetic pairs can be observed with larger probability. To make this point even stronger, we present Fig. 7, which shows similar coarse-grained results but for the electron and positron momenta, $|\mathbf{p}_{e^-}|$ and $|\mathbf{p}_{e^+}|$, respectively. The upper panel here

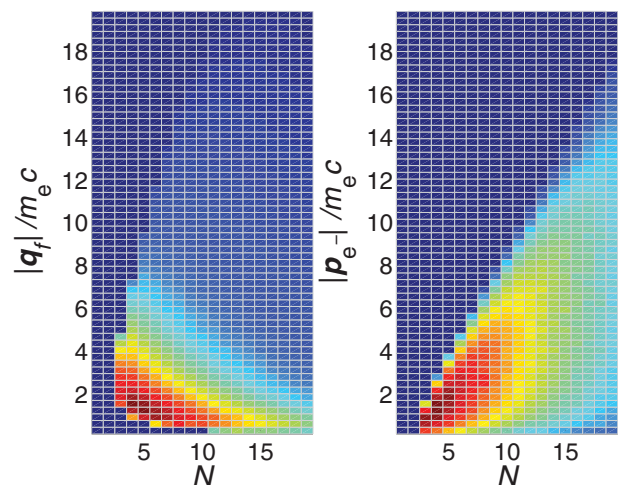


FIG. 6. (Color online) Coarse-grained differential probability rates of pair creation for the same laser-field parameters as in Fig. 2. While the left panel shows correlations between the number of absorbed laser photons N and the momentum transfer from the proton, $|\mathbf{q}_f|$, the right panel shows correlations between the number of photons N and the momentum gained by the electron, $|\mathbf{p}_{e^-}|$. The rates are raised to the power $1/10$ for a visual effect.

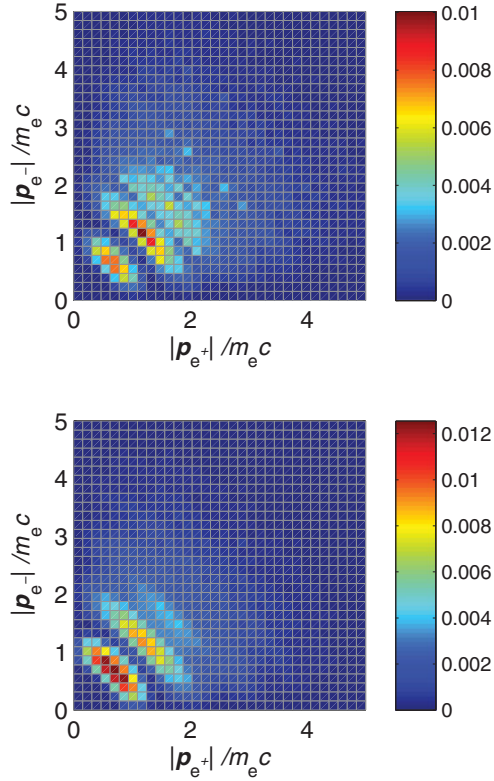


FIG. 7. (Color online) Coarse-grained differential probability rates of pair creation for the same laser-field parameters as in Fig. 2, showing correlations between the created electron, $|\mathbf{p}_{e-}|$, and positron, $|\mathbf{p}_{e+}|$, momenta. The upper panel is for the case when the proton recoil is taken into account, whereas the lower panel shows the results for the case when the proton recoil is neglected.

shows the mappings of the coarse-grained probability rates of pair creation calculated with an exact account for the proton recoil. The lower panel presents the results for the case when one disregards the recoil imparted on the proton. In both panels, the rates are averaged within square cells of dimension $20/128 \times 20/128$. In both panels, we see very distinct stripes that correspond to different photon numbers N , absorbed from the laser field during the pair production. In each case, the first stripe in the bottom left corner relates to the three-photon pair creation and is followed by the higher-photon order stripes. Comparing both panels of Fig. 7, we confirm that the energy delivered by the proton during its collision with the laser field results in producing more energetic pairs. In this case, the respective distribution is more spread toward higher electron and positron momenta. The maximum probability rate of pair creation is also shifted toward higher momenta of created particles, when the proton recoil is taken into account. In addition, we observe that the distributions presented in both panels of Fig. 7 are symmetric with respect to the electron and the positron momenta exchange, which is a general property of the S -matrix amplitude.

Now, we would like to compare the above results with the perturbative results obtained for the same frequency of the laser field $\omega = m_e c^2$ (in the chosen reference frame) but for a smaller intensity such that $\mu = 0.01$. In Fig. 8 we show the respective data. In the upper panel we present

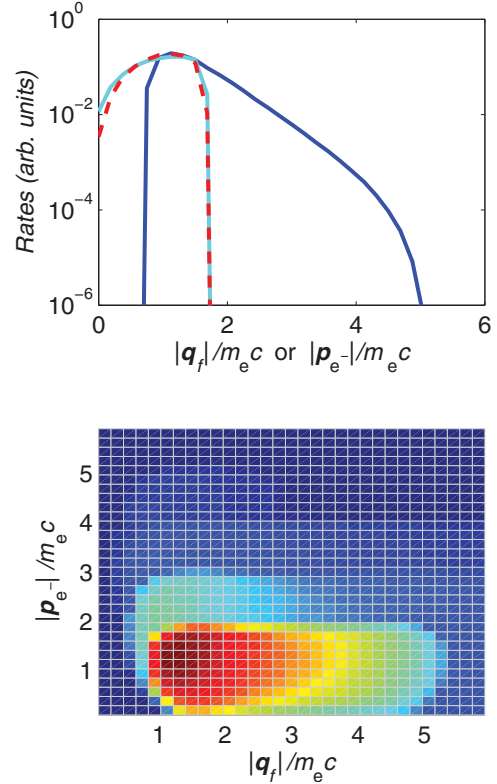


FIG. 8. (Color online) In the upper panel, we show the dependence of the probability rates of e^-e^+ pair creation on the momentum transfer from the colliding proton (solid blue line), or on the created electron (positron) momentum taking into account (dashed red line) or neglecting (solid cyan line) the proton recoil. Results are for the laser-field parameters, $\omega = m_e c^2$ (in the chosen reference frame) and $\mu = 0.01$, and for the lowest-order photon process ($N = 3$). In the lower panel, for the same laser-field parameters, we show the coarse-grained differential probability rates of electron-positron pair creation depending on the momentum delivered by the proton, $|\mathbf{q}_f|$, and on the electron (positron) momentum, $|\mathbf{p}_{e-}|$. The rates in the lower panel have been raised to the power $1/10$ for a visual purpose.

the partial rates for the lowest-order photon process that corresponds to three-photon absorption. The solid blue line shows the dependence of the rates on the momentum transfer from the colliding proton $|\mathbf{q}_f|$, whereas the dashed red line shows the dependence on the created electron (or positron) momentum $|\mathbf{p}_{e-}|$. As always, the results relate to the reference frame where the proton is at rest outside of the laser focus long before the collision. For a comparison, the solid cyan line shows the probability rates as a function of the electron (positron) momentum $|\mathbf{p}_{e-}|$ in the case when we treat the colliding proton as an infinitely massive particle, i.e., when we neglect its recoil. Even though the shapes of these lines are very similar, the absolute magnitudes of the corresponding rates, when multiplied by the value of the total probability rate of pair creation, do differ by roughly a factor of four. We see also that for the three-order photon process under consideration now, which is dominant in the present perturbative case of pair production, the corresponding rates are significant only for a nonzero momentum transfer from a target particle (solid blue line). Correspondingly, in the lower panel we show the

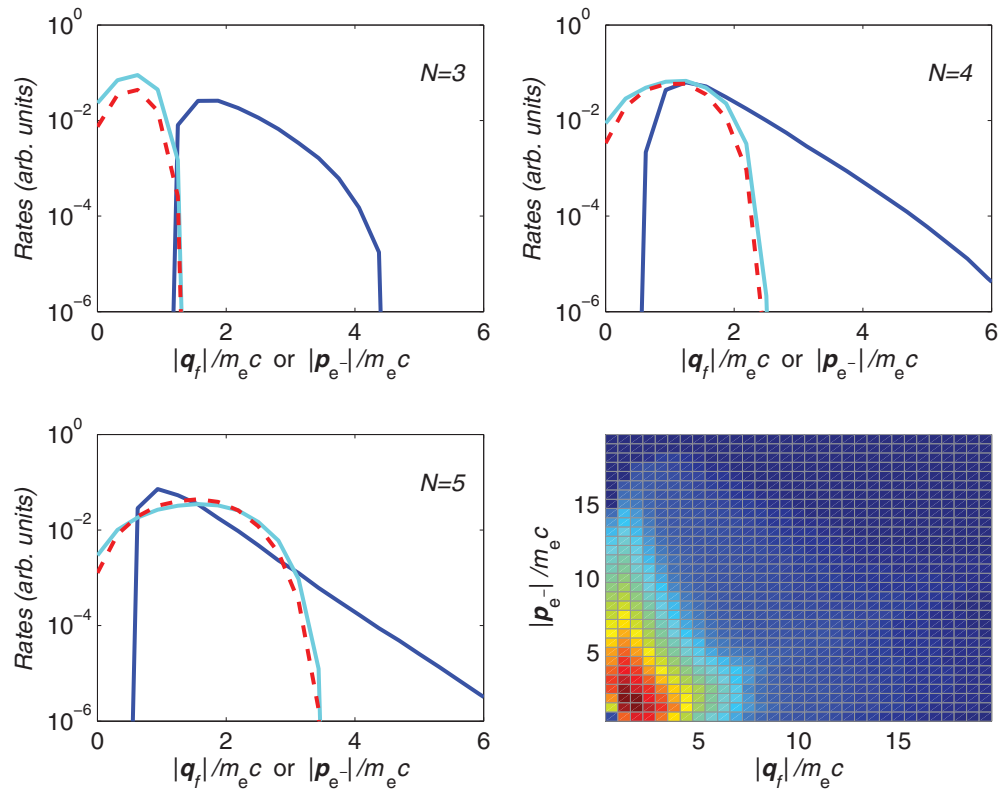


FIG. 9. (Color online) Same as in Fig. 8 but for different laser-field parameters, $\omega = m_e c^2$ (in the chosen reference frame) and $\mu = 1$. The partial rates which are presented correspond to three-, four-, and five-photon pair creation, as denoted in each panel.

coarse-grained differential probability rates of pair creation for the chosen laser parameters, showing the correlations between the electron (positron) momentum, $|p_{e^-}|$, and the momentum transfer from the colliding proton, $|q_f|$. The rates have been averaged within the square cells $6/32 \times 6/32$. We see from this panel, that even in the present perturbative case the e^-e^+ pair creation is most efficient when the momentum released by the proton during its collision with the laser beam is roughly within the range $m_e c$ to $2m_e c$. The same is observed in Fig. 9, in the lower right panel, which shows the coarse-grained differential probability rates of electron-positron pair creation [Eq. (11)] as a function of the momentum transferred by the proton during the collision with the laser beam and the momentum gained by the created electron, for the usual laser parameters used in this paper ($\omega = m_e c^2$ and $\mu = 1$). Even though the energy supplied by the proton is comparable in both these cases, nevertheless the pairs created by a stronger field (Fig. 9) are more energetic than the ones created by a weak field (Fig. 8). This follows from the fact that in the intermediate regime of pair creation the higher-order photon processes are favorable, resulting in producing more energetic pairs. In the remaining panels of Fig. 9 we present the partial rates of pair creation for $N = 3, 4$, and 5, using the same convention as in Fig. 8. As mentioned above, we observe that with increasing the number of absorbed laser photons N , more energetic pairs are produced. Analogous to Fig. 8, we note that qualitatively the partial rates as functions of the electron (positron) momentum $|p_{e^-}|$ for the case when we take into account the proton recoil (dashed red line), and we do not (solid cyan line) are very

similar, still slightly more distinct than for the perturbative case (Fig. 8). This distinction becomes more evident if we compare absolute values of the partial rates; while in the previous perturbative case the difference was by a factor of four, in the present nonperturbative case it is different by almost one order of magnitude. Going toward even more nonperturbative regime, one can find the respective difference to be increased.

At this point, let us refer to Ref. [32] where the authors have considered a perturbative regime of pair creation with $\mu = 7.5 \times 10^{-4}$ and circular polarization of the laser field. As has been shown there, for such low μ the recoil effects are negligibly small. One can see in this section that the recoil effects are already evident, though they are not very pronounced, for the linearly polarized laser field and for $\mu = 0.01$, which is still in the perturbative regime. The point is, that the recoil effects modify the probability rates of pair creation, and these modifications become more pronounced with increasing μ , i.e., with increasing the laser field intensity (see also Fig. 1 and similar figures in Refs. [34,38]). One may conclude therefore that already $\mu = 0.01$ is not sufficiently deep into the perturbative regime of pair creation for recoil to be completely negligible.

For completeness, let us mention other features that distinguish between the very few- and the very many-photon pair creation processes. In the present paper and in the work by Müller and Müller [32], the differential partial probability rates of pair creation are very smooth functions of the momentum transfer supplied by a target particle. This is in contrast to our most recent works on the tunneling electron-positron

pair creation [34,38], where we have observed very rapid and dense oscillations of the corresponding rates. This can be explained as interferences between a large number of amplitudes that relate to different elementary processes with a specific sequence of absorbed and emitted by the target particle laser photons (for details, see Ref. [34]). This is not the case any longer for few-photon processes. Let us recall that in the same paper [34], we have observed a very dramatic dependence of the probability rates of pair creation on the laser-field polarization. In particular, only for a linearly polarized laser field have the respective rates turned out to be significant. Let us note that in this case the above-mentioned amplitudes are defined in terms of the generalized Bessel functions, which, for large N , vanish abruptly for polarization of the laser field different than linear. On the other hand, for small N , which correspond to few-photon processes, the generalized Bessel functions smoothly change with varying the ellipticity parameter of the laser field. Even though we do not present the respective results here, we have performed calculations for the circular polarization and the same parameters of the field as the ones considered in this paper. We have found a very similar qualitative behavior of the probability rates of e^-e^+ pair creation in both these cases.

VII. CONCLUSIONS

In the present paper, the results for electron-positron pair creation in the head-on laser-beam-proton collisions that account for or disregard the proton finite mass have been presented. We have focused on the above-threshold regime of pair production, even though for a comparison we have also presented the results for the perturbative multiphoton regime of the process.

In contrast to Ref. [32], where dominant first-order photon processes of the multiphoton e^-e^+ pair creation were considered, we have analyzed here the full above-threshold-photon spectra. As typical for the ATI process, we have observed a nonmonotonic behavior of the partial probability rates of pair creation with increasing the number of absorbed laser photons N . It follows from our results that the maximum of partial rates is observed for a nonzero momentum transfer from the colliding proton. For the parameters considered in this paper, we have obtained up to one order of magnitude increase of the total probability rates of pair creation when the proton recoil is accounted for. In addition, we have observed that more energetic electrons and positrons are created if extra energy is supplied during a relativistic proton impact on the intense laser field. Comparing these results with the results obtained for the multiphoton case, we clearly see that the recoil effects become more important with increasing the parameter μ , i.e., when going into the nonperturbative regime of laser-matter interaction.

In closing, let us remind readers that currently the most energetic proton beams are obtained in the Large Hadron Collider facility at CERN, gaining energies up to 7 TeV. Assuming the Lorentz factor of $\gamma \simeq 7000$, which corresponds to these most energetic protons, an intense laser working in the extreme ultraviolet (XUV) regime is necessary to test our theoretical predictions presented in this paper. To be more specific, lasers working in the frequency domain of around 40 eV and intensity 10^{21} W/cm² are necessary in the respective experimental setup. Let us note that such, or even higher, intensities were already reported for a near-optical regime [8]. They are also predicted for future XUV laser sources, as based on higher-order harmonic generation from solid surfaces [72,73].

-
- [1] M. Marklund and P. Shukla, *Rev. Mod. Phys.* **78**, 591 (2006).
 [2] Y. I. Salamin, S. X. Hu, K. Z. Hatsagortsyan, and C. H. Keitel, *Phys. Rep.* **427**, 41 (2006).
 [3] F. Ehlötzky, K. Krajewska, and J. Z. Kamiński, *Rep. Prog. Phys.* **72**, 046401 (2009).
 [4] F. Sauter, *Z. Phys.* **69**, 742 (1931).
 [5] J. Schwinger, *Phys. Rev.* **82**, 664 (1951).
 [6] E. Brezin and C. Itzykson, *Phys. Rev. D* **2**, 1191 (1970).
 [7] V. S. Popov, *Zh. Eksp. Teor. Fiz.* **61**, 1334 (1971) [*Sov. Phys. JETP* **34**, 709 (1972)].
 [8] G. A. Mourou, T. Tajima, and S. V. Bulanov, *Rev. Mod. Phys.* **78**, 309 (2006).
 [9] V. Yanovsky, V. Chvykov, G. Kalinchenko, P. Rousseau, T. Planchon, T. Matsuoka, A. Maksimchuk, J. Nees, G. Cheriaux, and K. Krushelnick, *Opt. Express* **16**, 2109 (2008).
 [10] See the online proposal at [<http://www.eli-laser.eu>].
 [11] M. Boca and V. Florescu, *Phys. Rev. A* **80**, 053403 (2009).
 [12] M. Boca and V. Florescu, *Eur. Phys. J. D* **61**, 446 (2011).
 [13] D. Seipt and B. Kämpfer, *Phys. Rev. A* **83**, 022101 (2011).
 [14] F. Mackenroth and A. Di Piazza, *Phys. Rev. A* **83**, 032106 (2011).
 [15] M. Boca and A. Oprea, *Phys. Scr.* **83**, 055404 (2011).
 [16] H. A. Jivanyan, *J. Phys. B* **44**, 055401 (2011).
 [17] V. P. Yakovlev, *Zh. Eksp. Teor. Fiz.* **49**, 318 (1965) [*Sov. Phys. JETP* **22**, 223 (1966)].
 [18] M. H. Mittleman, *Phys. Rev. A* **35**, 4624 (1987).
 [19] E. P. Liang, S. C. Wilks, and M. Tabak, *Phys. Rev. Lett.* **81**, 4887 (1998).
 [20] C. Müller, A. B. Voitkiv, and N. Grün, *Phys. Rev. A* **67**, 063407 (2003).
 [21] C. Müller, A. B. Voitkiv, and N. Grün, *Phys. Rev. Lett.* **91**, 223601 (2003).
 [22] C. Müller, A. B. Voitkiv, and N. Grün, *Phys. Rev. A* **70**, 023412 (2004).
 [23] P. Sieczka, K. Krajewska, J. Z. Kamiński, P. Panek, and F. Ehlötzky, *Phys. Rev. A* **73**, 053409 (2006).
 [24] J. Z. Kamiński, K. Krajewska, and F. Ehlötzky, *Phys. Rev. A* **74**, 033402 (2006).
 [25] K. Krajewska, J. Z. Kamiński, and F. Ehlötzky, *Laser Phys.* **16**, 272 (2006).
 [26] A. I. Milstein, C. Müller, K. Z. Hatsagortsyan, U. D. Jentschura, and C. H. Keitel, *Phys. Rev. A* **73**, 062106 (2006).
 [27] M. Yu. Kuchiev and D. J. Robinson, *Phys. Rev. A* **76**, 012107 (2007).
 [28] K. Krajewska and J. Z. Kamiński, *Laser Phys.* **18**, 185 (2008).

- [29] C. Deneke and C. Müller, *Phys. Rev. A* **78**, 033431 (2008).
- [30] C. Müller, *Phys. Lett. B* **672**, 56 (2009).
- [31] E. Lötstedt, U. D. Jentschura, and C. H. Keitel, *New J. Phys.* **11**, 013054 (2009).
- [32] S. J. Müller and C. Müller, *Phys. Rev. D* **80**, 053014 (2009).
- [33] A. Di Piazza, E. Lötstedt, A. I. Milstein, and C. H. Keitel, *Phys. Rev. A* **81**, 062122 (2010).
- [34] K. Krajewska and J. Z. Kamiński, *Phys. Rev. A* **82**, 013420 (2010). In Eq. (31) instead of $1/(2\pi^3)$, it should be $4(2\pi)^6$. This misprint has no influence on the following formulas and the numerical results presented there.
- [35] H. Hu, C. Müller, and C. H. Keitel, *Phys. Rev. Lett.* **105**, 080401 (2010).
- [36] A. Di Piazza, A. I. Milstein, and C. Müller, *Phys. Rev. A* **82**, 062110 (2010).
- [37] T.-O. Müller and C. Müller, *Phys. Lett. B* **696**, 201 (2011).
- [38] K. Krajewska, *Laser Phys.* **21**, 1275 (2011).
- [39] H. R. Reiss, *J. Math. Phys.* **3**, 59 (1962).
- [40] L. S. Brown and T. W. B. Kibble, *Phys. Rev.* **133**, A705 (1964).
- [41] A. I. Nikishov and V. I. Ritus, *Zh. Eksp. Teor. Fiz.* **46**, 776 (1964) [*Sov. Phys. JETP* **19**, 529 (1964)].
- [42] N. B. Narozhny, A. I. Nikishov, and V. I. Ritus, *Zh. Eksp. Teor. Fiz.* **47**, 930 (1964) [*Sov. Phys. JETP* **20**, 622 (1965)].
- [43] N. B. Narozhny and M. S. Fofanov, *Laser Phys.* **7**, 141 (1997).
- [44] V. S. Popov, *Pis'ma Zh. Eksp. Teor. Fiz.* **74**, 151 (2001) [*JETP Lett.* **74**, 133 (2001)].
- [45] A. Ringwald, *Phys. Lett. B* **510**, 107 (2001).
- [46] H. K. Avetissian, A. K. Avetissian, G. F. Mkrtchian, and K. V. Sedrakian, *Phys. Rev. E* **66**, 016502 (2002).
- [47] A. Di Piazza, *Phys. Rev. D* **70**, 053013 (2004).
- [48] D. B. Blaschke, A. V. Prozorkevich, C. D. Roberts, S. M. Schmidt, and S. A. Smolyansky, *Phys. Rev. Lett.* **96**, 140402 (2006).
- [49] A. R. Bell and J. G. Kirk, *Phys. Rev. Lett.* **101**, 200403 (2008).
- [50] G. R. Mocken, M. Ruf, C. Müller, and C. H. Keitel, *Phys. Rev. A* **81**, 022122 (2010).
- [51] S. S. Bulanov, V. D. Mur, N. B. Narozhny, J. Nees, and V. S. Popov, *Phys. Rev. Lett.* **104**, 220404 (2010).
- [52] D. L. Burke *et al.*, *Phys. Rev. Lett.* **79**, 1626 (1997).
- [53] C. Bamber *et al.*, *Phys. Rev. D* **60**, 092004 (1999).
- [54] V. S. Popov, *Zh. Eksp. Teor. Fiz.* **63**, 1586 (1972) [*Sov. Phys. JETP* **36**, 840 (1973)].
- [55] V. I. Ritus, *J. Rus. Laser Res.* **6**, 497 (1985).
- [56] C. Müller, K. Z. Hatsagortsyan, M. Ruf, S. J. Müller, H. G. Hetzheim, M. C. Kohler, and C. H. Keitel, *Laser Phys.* **19**, 1743 (2009).
- [57] L. V. Keldysh, *Zh. Eksp. Teor. Fiz.* **47**, 1945 (1964) [*Sov. Phys. JETP* **20**, 1307 (1965)].
- [58] V. P. Oleinik, *Zh. Eksp. Teor. Fiz.* **52**, 1049 (1967) [*Sov. Phys. JETP* **25**, 697 (1967)].
- [59] V. P. Oleinik and I. V. Belousov, *The Problems of Quantum Electrodynamics of the Vacuum, Dispersive Media and Strong Fields* (Kishinev, Shtiintsa, 1983).
- [60] S. P. Roshchupkin, *Laser Phys.* **6**, 837 (1996).
- [61] P. Agostini, F. Fabre, G. Mainfray, G. Petite, and N. K. Rahman, *Phys. Rev. Lett.* **42**, 1127 (1979).
- [62] L. F. DiMauro and P. Agostini, *Adv. At. Mol. Opt. Phys.* **35**, 79 (1995).
- [63] M. Protopapas, C. H. Keitel, and P. L. Knight, *Rep. Prog. Phys.* **60**, 389 (1997).
- [64] N. B. Delone and V. P. Krainov, *Usp. Fiz. Nauk* **168**, 531 (1998) [*Sov. Phys. Usp.* **41**, 469 (1998)].
- [65] W. Becker, F. Grasbon, R. Kopold, D. B. Milošević, G. G. Paulus, and H. Walther, *Adv. At. Mol. Opt. Phys.* **48**, 35 (2002).
- [66] K. J. Schafer, B. Yang, L. F. DiMauro, and K. C. Kulander, *Phys. Rev. Lett.* **70**, 1599 (1993).
- [67] P. B. Corkum, *Phys. Rev. Lett.* **71**, 1994 (1993).
- [68] P. Kruit, J. Kimman, H. G. Muller, and M. J. van der Wiel, *Phys. Rev. A* **28**, 248 (1983).
- [69] L. A. Lompre, A. Huillier, G. Mainfray, and C. Manus, *J. Opt. Soc. Am. B* **2**, 1906 (1985).
- [70] L. A. Lompre, G. Mainfray, C. Manus, and J. Kupersztych, *J. Phys. B* **20**, 1009 (1987).
- [71] G. Petite, P. Agostini, and F. Yergeau, *J. Opt. Soc. Am. B* **4**, 765 (1987).
- [72] A. Pukhov, *Nature Phys.* **2**, 439 (2006).
- [73] B. Dromey *et al.*, *Nature Phys.* **5**, 146 (2009).